The *Fermi* LAT and WMAP view of particle acceleration in supernova remnant HB 21

G.Pivato, J.W.Hewitt, and L.Tibaldo
INFN and University of Padova
pivato@pd.infn.it

on behalf of the *Fermi* LAT collaboration

Turku, July 11-12, 2013

Outline

- ⇒ Background on supernova remnant HB 21
- ⇒ *Fermi* LAT analysis
  - ↪ morphological analysis
  - ↪ spectral analysis
  - ↪ spectral variations across the remnant
- ⇒ WMAP analysis
- ⇒ Nonthermal modeling
  - ↪ physical environment and emission mechanism
  - ↪ one-zone model
  - ↪ two-zone model
  - ↪ comparison with other SNRs
- ⇒ Conclusions

Background on supernova remnant HB 21

HB21

⇒ Radio coordinates: l=89.°0, b=4.°9 (Green D.A., 2009)

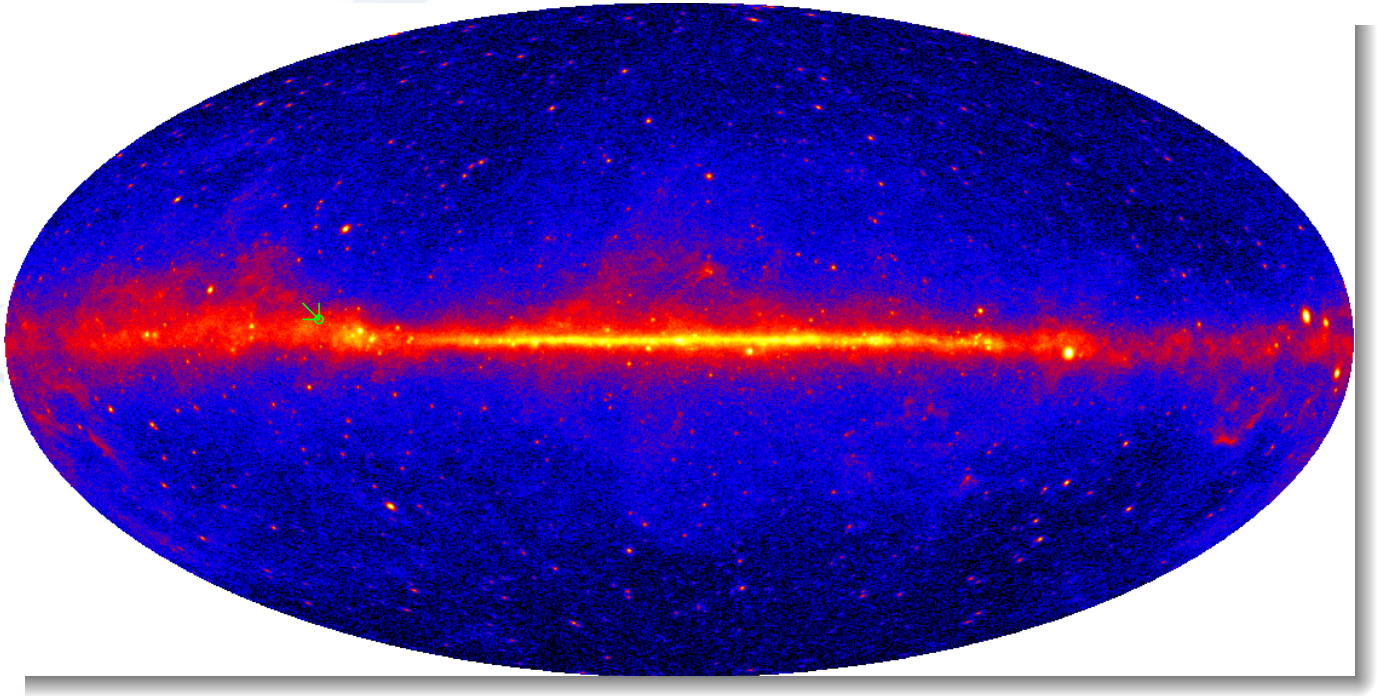

Background on supernova remnant HB 21

HB21

- ⇒ Radio coordinates: l=89.°0, b=4.°9 (Green D.A., 2009)
- ⇒ Mixed morphology
- ⇒ age $\sim 10^4$ yr (Flower & Pineau des Forêts, 1999)
- ⇒ distance $\sim$ 1.7 kpc (Byun et al., 2006)

distance problem

- ↪ estimation by Tatematsu et al. (1990): $\sim$ 0.8 kpc adopted in Reichardt et al. (2012) paper
- ↪ estimation by Byun et al. (2006): $\sim$ 1.7 kpc adopted in this work

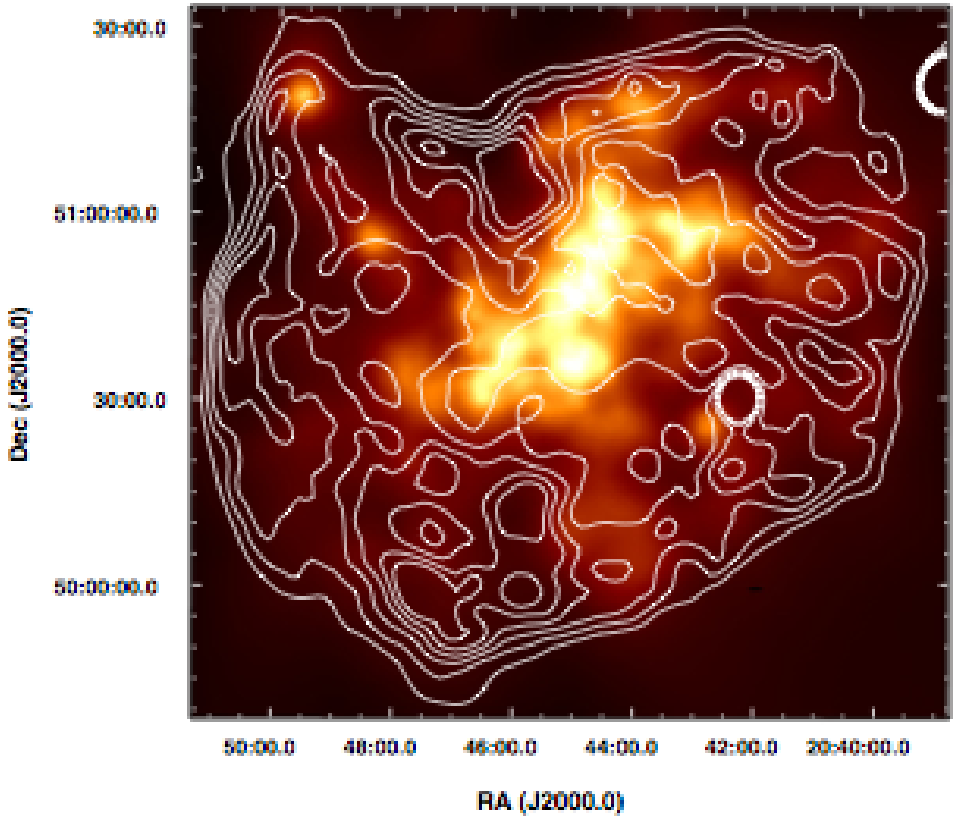

Figure 2. Mosaicked *ROSAT* PSPC image of HB21: we have superposed the same radio contours as in Figure 1. The intensity range of this image is 10^{-4}–2.1×10^{-2} counts s^{-1} $arcmin^{-2}$.

rom Pannuti et al., The Astronomical Journal, 140, 2010 December

Background on supernova remnant HB 21

HB21

- ⇒ Radio coordinates: l=89.°0, b=4.°9 (Green D.A., 2009)
- ⇒ Mixed morphology
- ⇒ age $\sim 10^4$ yr (Flower & Pineau des Forêts, 1999)
- ⇒ distance $\sim$ 1.7 kpc (Byun et al., 2006)
- ⇒ interacting with molecular clouds

from Koo et al.,
The Astrophysical Journal, 552, May 2001

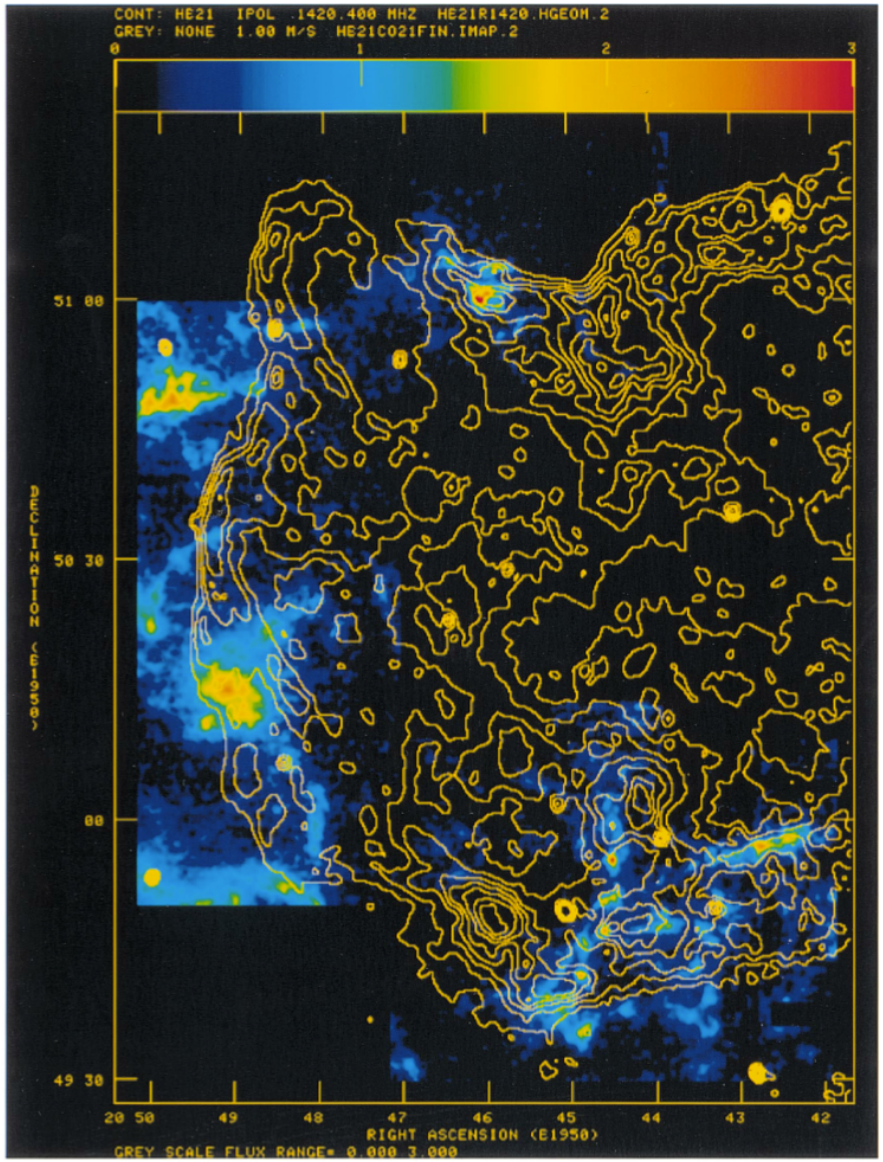

FIG. 1.—^{12}CO $J = 2$–1 integrated intensity map of HB 21. The velocity range is from $v_{LSR} = +3.9$ to -17.5 km s^{-1}, and the integrated intensity varies from 0 to 64 K km s^{-1}. Overlaid contour map shows the 1420 MHz brightness distribution of HB 21 obtained by T90 using the TRAO synthesis telescope.

Morphological analysis

Models compared

- ⇒ Four point sources
- ⇒ disk (with and without 2FGL J2051.8+5054)

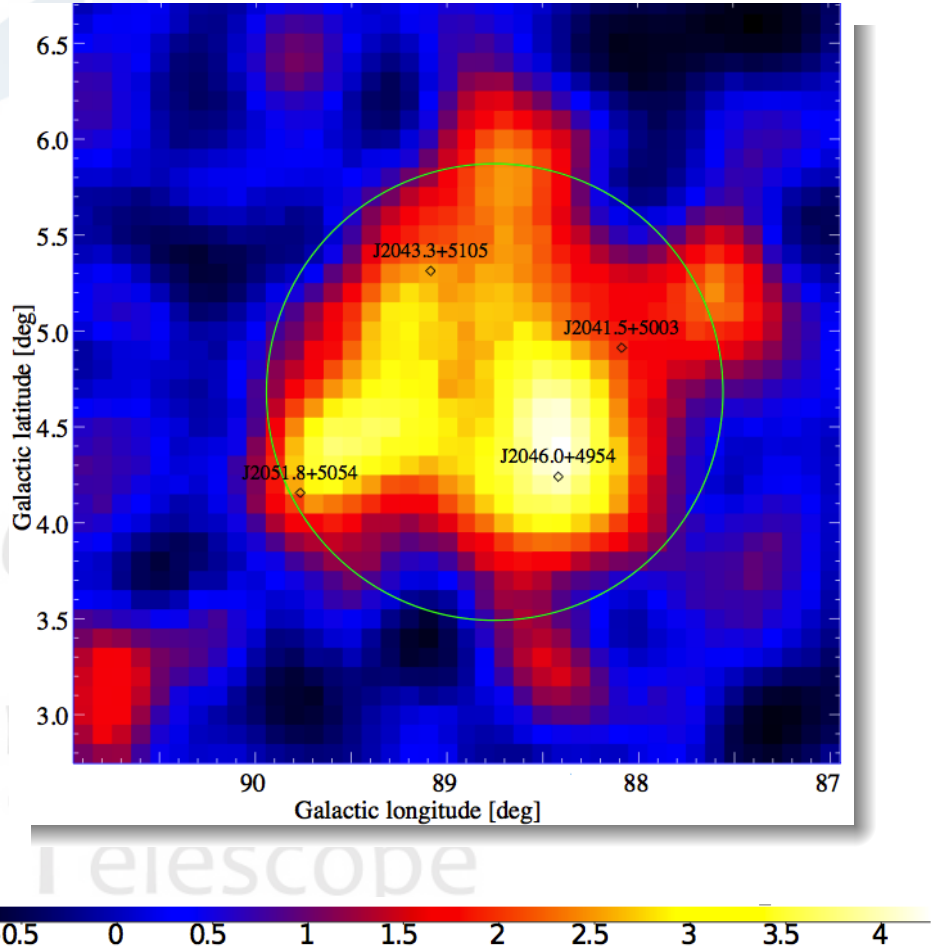

γ image from 1 GeV to 300 GeV background subtracted

Morphological analysis

Models compared

- ⇒ Four point sources
- ⇒ disk (with and without 2FGL J2051.8+5054)
- ⇒ radio emitting region

from Sino-German Telescope (Gao et al., 2011)
Radio emission intensity at 6 cm

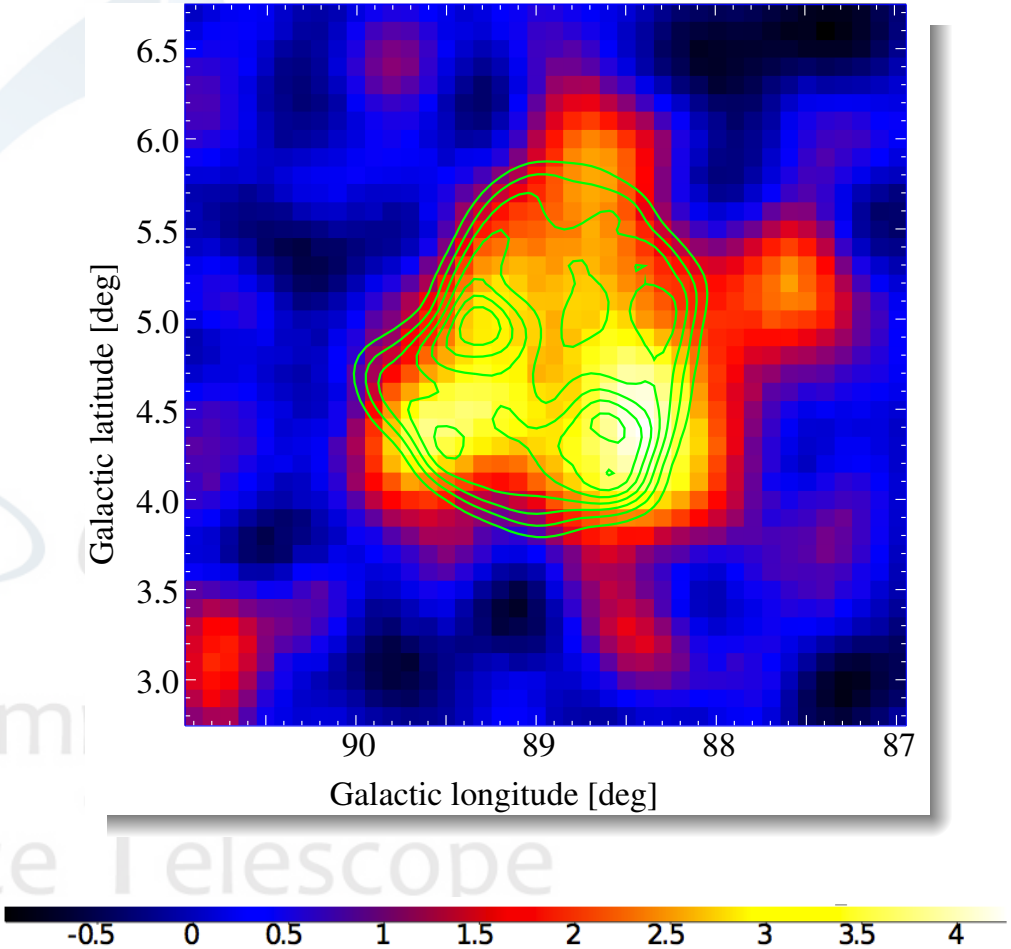

γ image from 1 GeV to 300 GeV background subtracted

Morphological analysis

Models compared

- ⇒ Four point sources
- ⇒ disk (with and without 2FGL J2051.8+5054)
- ⇒ radio emitting region
- ⇒ X-ray emitting region

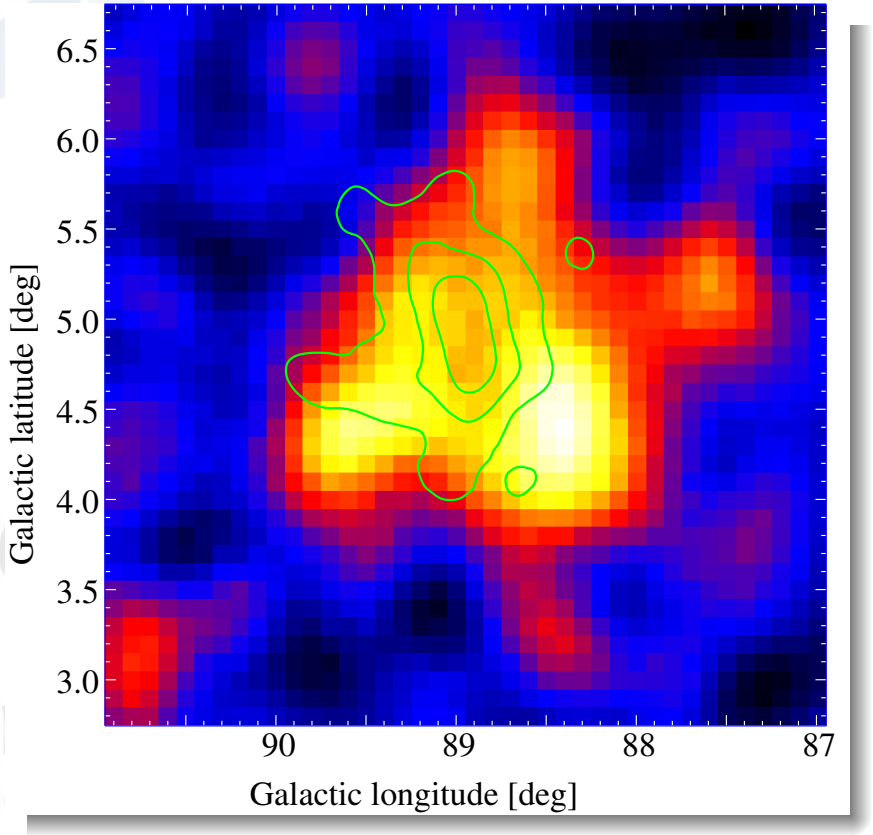

Background-subtracted ROSAT X-ray emission

γ image from 1 GeV to 300 GeV background subtracted

Morphological analysis

Models compared

- ⇒ Four point sources
- ⇒ disk (with and without 2FGL J2051.8+5054)
- ⇒ radio emitting region
- ⇒ X-ray emitting region

Sources	TS	dof
Null hypothesis	0	0
4 point sources	256	10
disk	302	5
disk + 2FGL J2051.8+5054	316	7
X-ray image	212	2
radio image	298	2

Best fit disk parameters

- ⇒ (l,b)=($88.^\circ 75 \pm 0.^\circ 04$, $4.^\circ 65 \pm 0.^\circ 06$)
- ⇒ $r = 1.^\circ 19 \pm 0.^\circ 06$

Spectral analysis

Models compared

- ⇒ curved spectrum
- ⇒ statistic errors
- ⇒ systematic errors

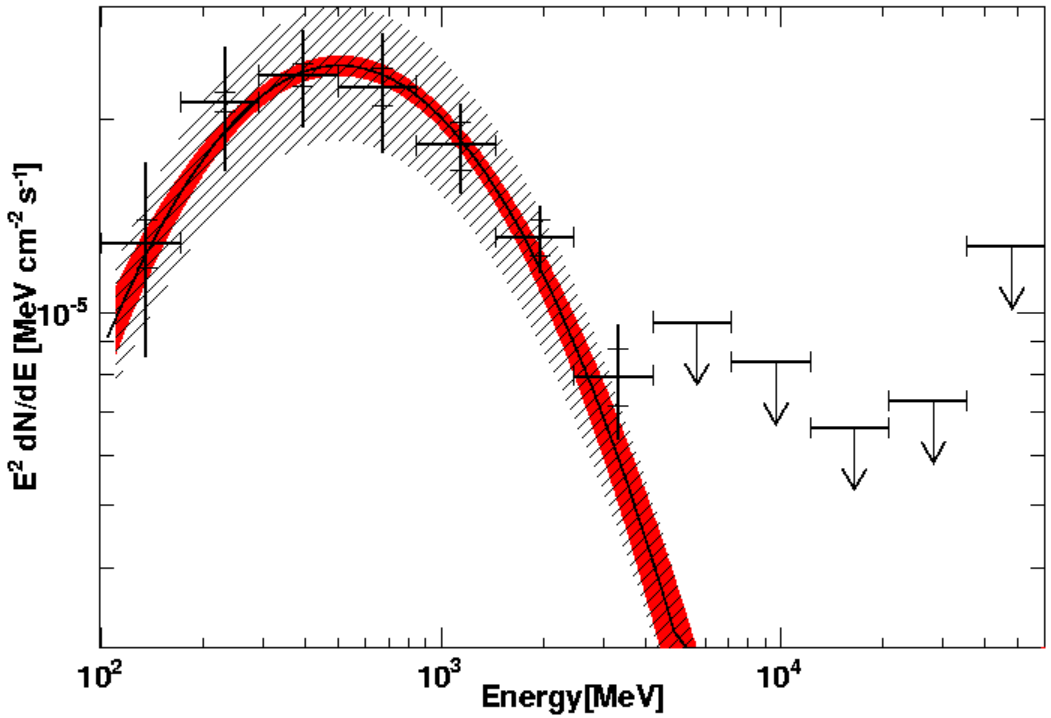

spectrum shape	ΔTS	dof
power law	0	0
log-parabola	92	1
smooth broken power law	41	2
power law with exponential cutoff	82	1

Spectral variations across the remnant

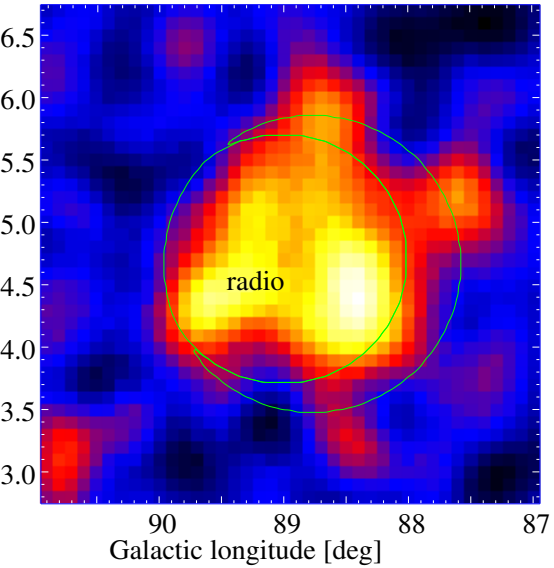

Analysis performed for $E > 1$ GeV.
If $E > 100$ MeV, results are consistent.

partition	ΔTS	d.o.f.
single disk	0	0
radio	2.8	2

Spectral variations across the remnant

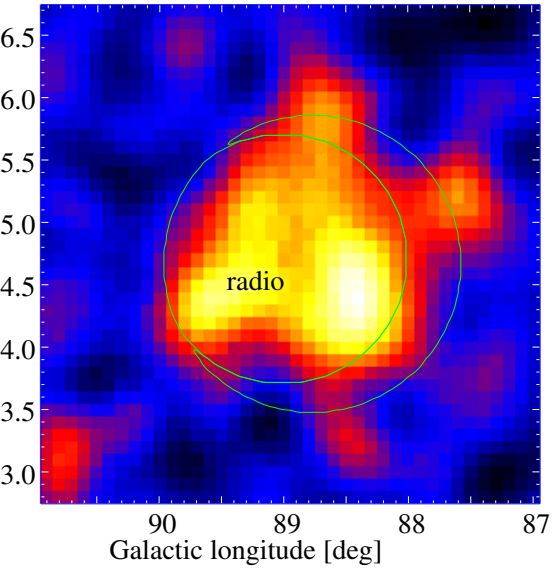

Analysis performed for $E > 1$ GeV.
If $E > 100$ MeV, results are consistent.

partition	ΔTS	d.o.f.
single disk	0	0
radio	2.8	2
shocked CO	4.2	2

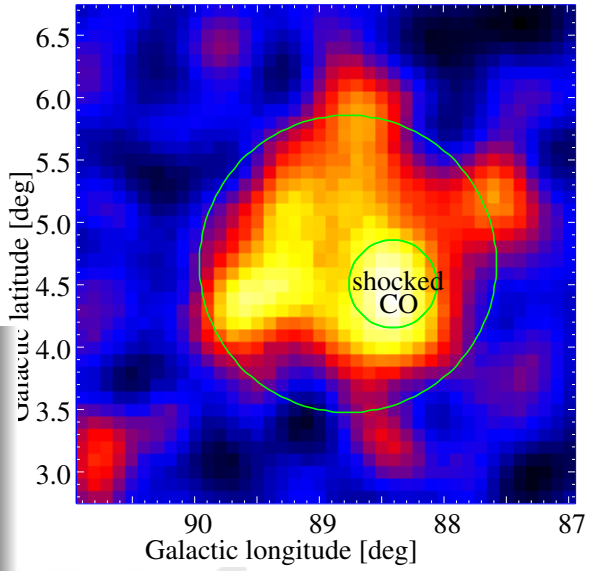

Spectral variations across the remnant

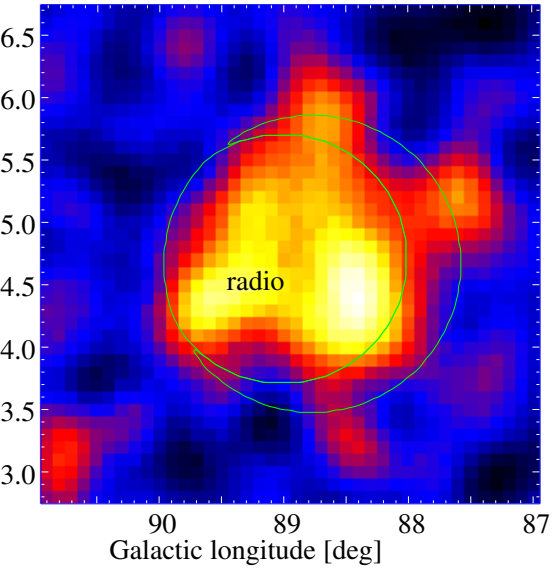

Analysis performed for $E > 1$ GeV.
If $E > 100$ MeV, results are consistent.

partition	ΔTS	d.o.f.
single disk	0	0
radio	2.8	2
shocked CO	4.2	2
split CO	2.2	2

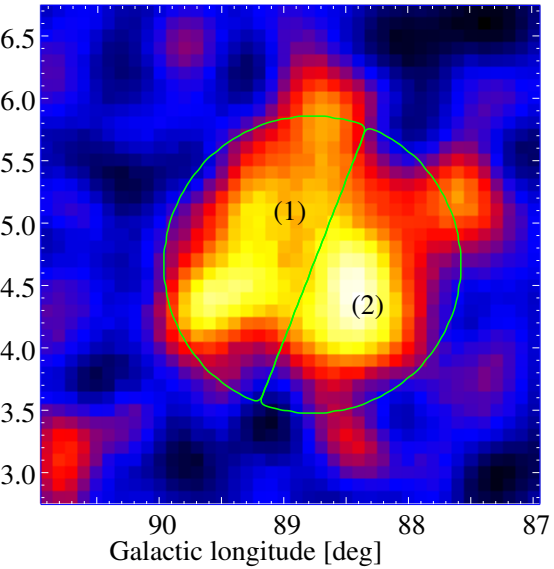

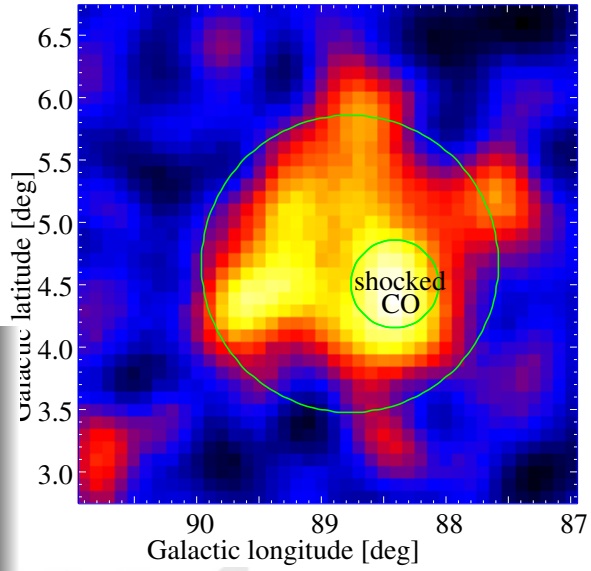

Spectral variations across the remnant

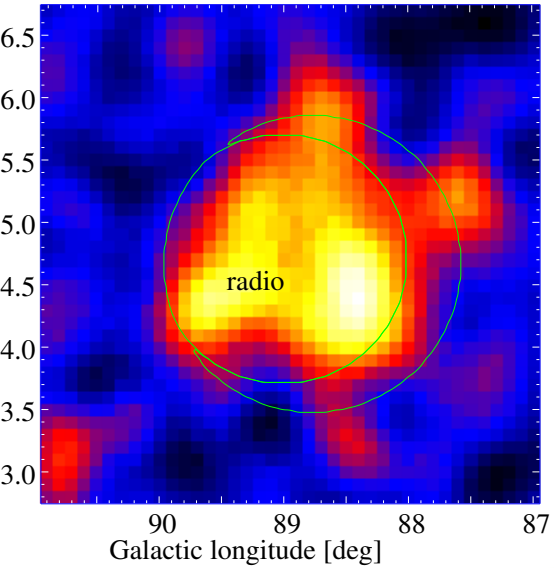

Analysis performed for $E > 1$ GeV.
If $E > 100$ MeV, results are consistent.

partition	ΔTS	d.o.f.
single disk	0	0
radio	2.8	2
shocked CO	4.2	2
split CO	2.2	2
3 regions	1.6	4

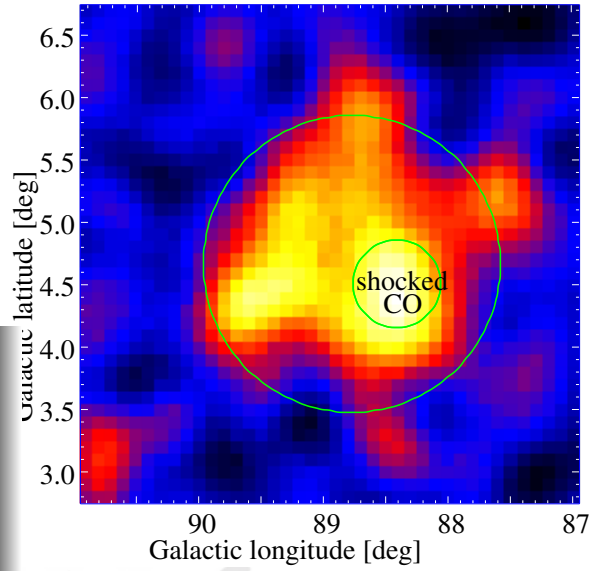

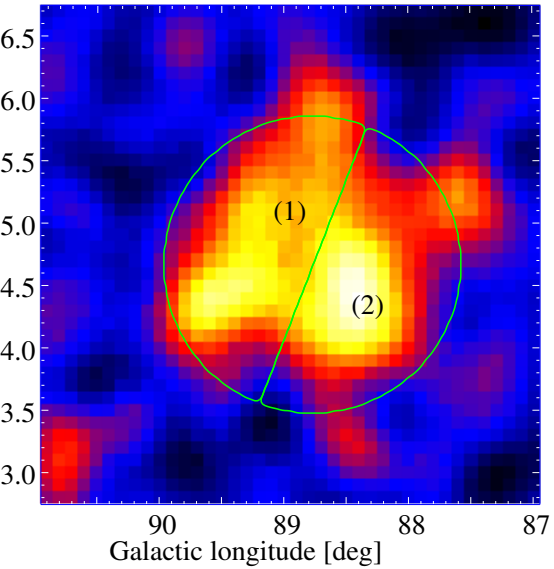

Reichardt et al. (2012) find a 2σ spectral variation for slice (1) not seen in our analysis

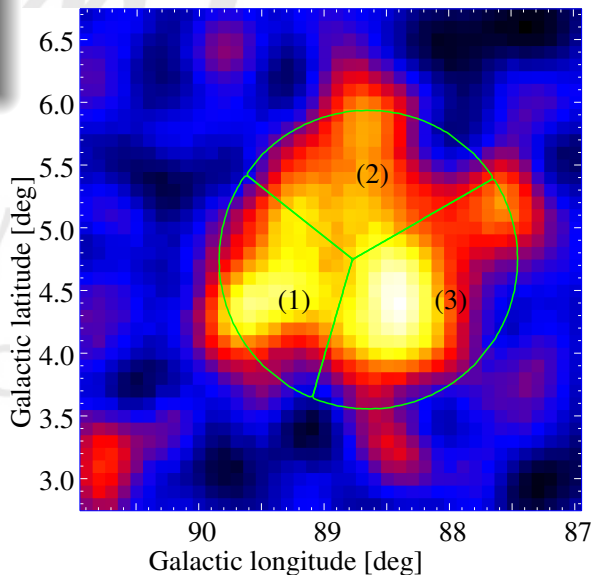

Spectral variations across the remnant

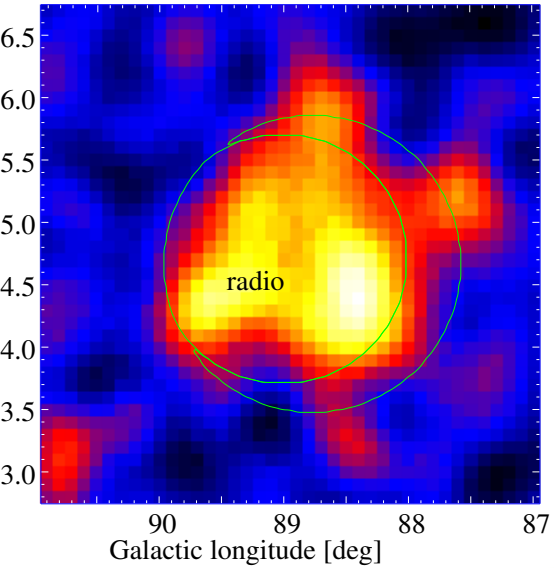

Analysis performed for $E > 1$ GeV.
If $E > 100$ MeV, results are consistent.

partition	ΔTS	d.o.f.
single disk	0	0
radio	2.8	2
shocked CO	4.2	2
split CO	2.2	2
3 regions	1.6	4

No spectral variations found

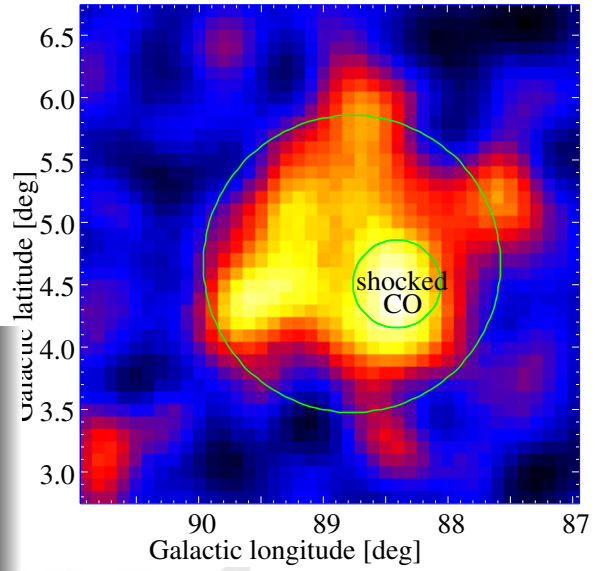

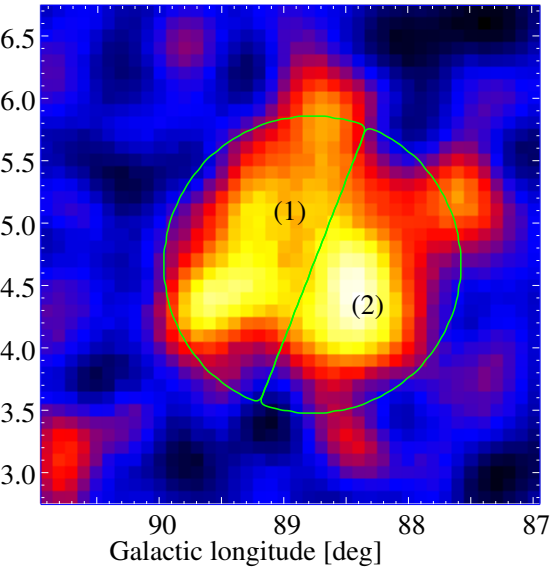

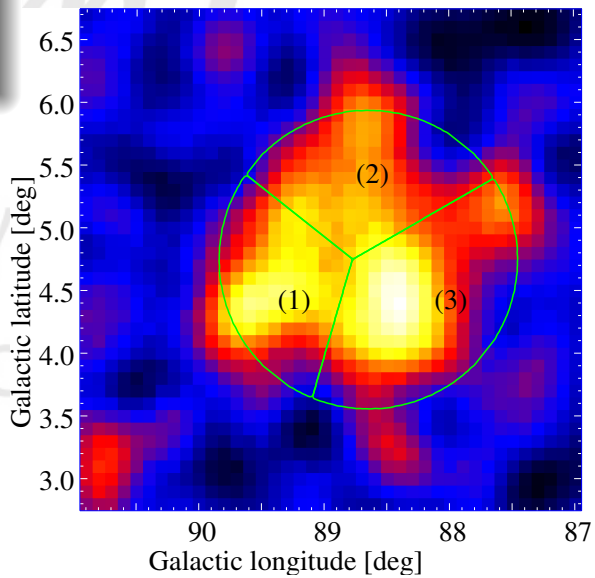

WMAP analysis

Radio analysis

⇒ point source 3C 418 removed

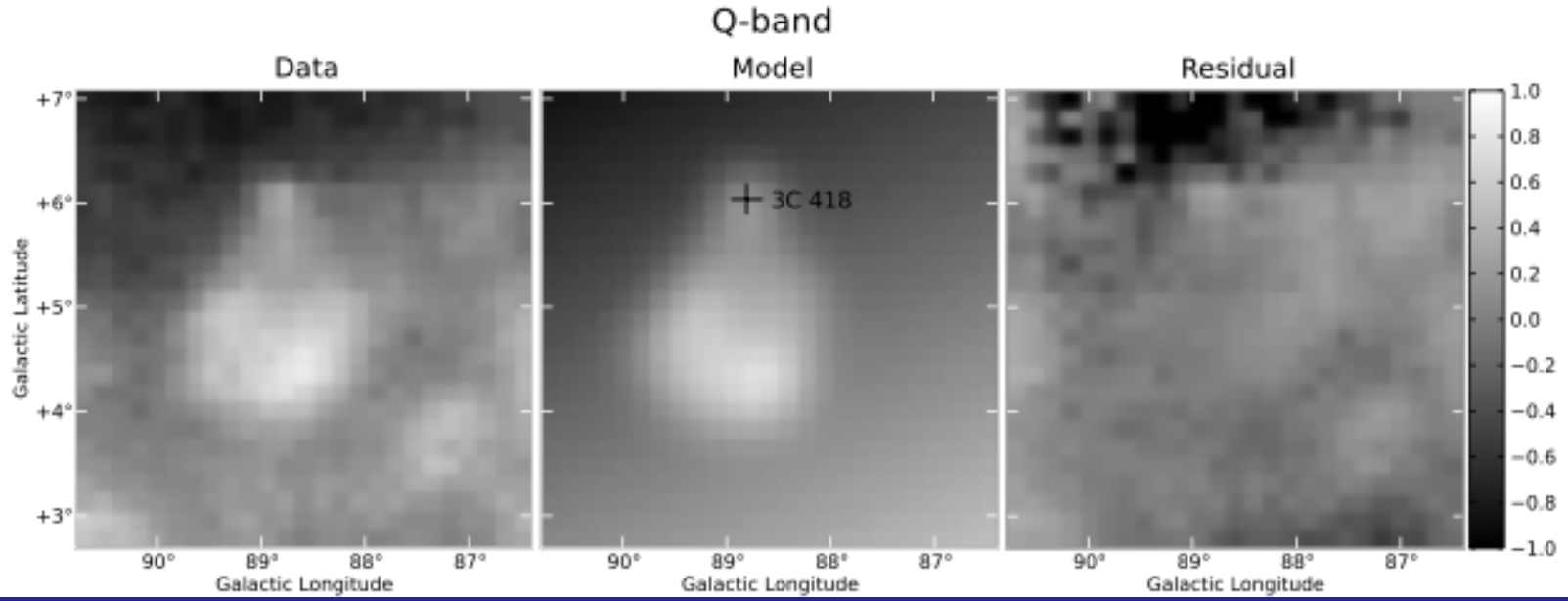

WMAP analysis

Radio analysis

- ⇒ point source 3C 418 removed
- ⇒ global radio spectrum from 38 MHz to 61 GHz

flux obtained with radio template at 6 cm from Sino-German Telescope (Gao et al., 2011)

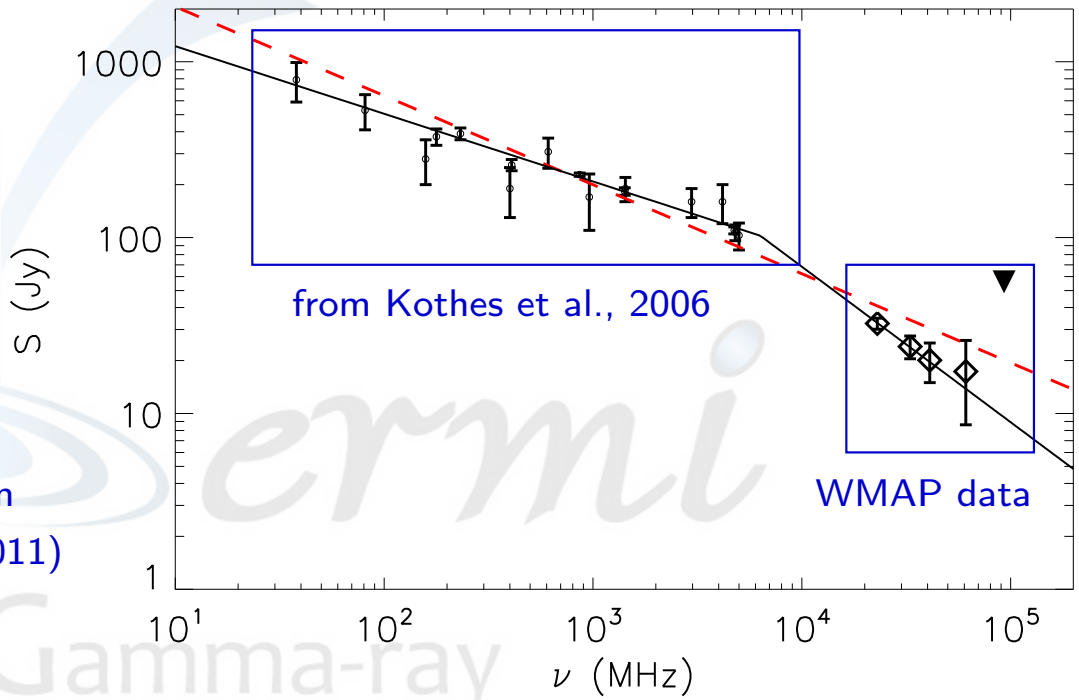

Radio spectral index below 10 GHz from the entire remnant = 0.38

WMAP analysis

Radio analysis

- ⇒ point source 3C 418 removed
- ⇒ global radio spectrum from 38 MHz to 61 GHz
- ⇒ spectral break significance: 5.3σ

flux obtained with radio template at 6 cm from Sino-German Telescope (Gao et al., 2011)

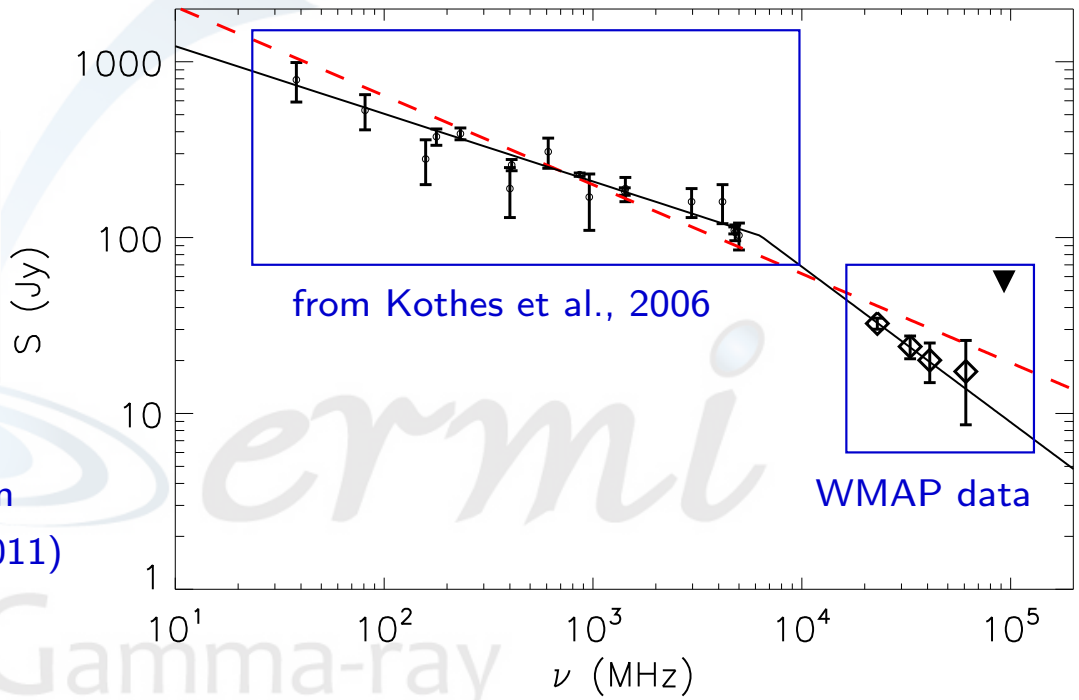

break cannot be explained by spectral variations across HB 21

Physical environment and emission mechanism

Physical environment around HB 21

- ⇒ HB 21 lies in the vicinity of molecular clouds
- ⇒ [S II] but no [O III] ⇒ $v_{shock} < 100$ km s^{-1}, densities 2.5 cm^{-3} (Mavromatakis et al., 2007)
- ⇒ shocked CO filaments (densities $\sim 10^2 - 10^4$ cm^{-3} and filling factors ≤ 0.1, Koo et al., 2001)
- ⇒ HI density for expanding shell: ~ 8 cm^{-3} (Koo et Heiles, 1991)
- ⇒ maximum density (volume-average) = 25 cm^{-3}

Physical environment and emission mechanism

Physical environment around HB 21

- ⇒ HB 21 lies in the vicinity of molecular clouds
- ⇒ [S II] but no [O III] ⇒ $v_{shock} < 100$ km s^{-1}, densities 2.5 cm^{-3} (Mavromatakis et al., 2007)
- ⇒ shocked CO filaments (densities $\sim 10^2 - 10^4$ cm^{-3} and filling factors ≤ 0.1, Koo et al., 2001)
- ⇒ HI density for expanding shell: ~ 8 cm^{-3} (Koo et Heiles, 1991)
- ⇒ maximum density (volume-average) = 25 cm^{-3}

Emission mechanism

- ⇒ hadronic scenario
- ⇒ leptonic scenario

Physical environment and emission mechanism

Physical environment around HB 21

- ⇒ HB 21 lies in the vicinity of molecular clouds
- ⇒ [S II] but no [O III] ⇒ $v_{shock} < 100$ km s^{-1}, densities 2.5 cm^{-3} (Mavromatakis et al., 2007)
- ⇒ shocked CO filaments (densities $\sim 10^2 - 10^4$ cm^{-3} and filling factors ≤ 0.1, Koo et al., 2001)
- ⇒ HI density for expanding shell: ~ 8 cm^{-3} (Koo et Heiles, 1991)
- ⇒ maximum density (volume-average) = 25 cm^{-3}

Emission mechanism

- ⇒ hadronic scenario
  - ↪ π^0-decay
- ⇒ leptonic scenario

Physical environment and emission mechanism

Physical environment around HB 21

- ⇒ HB 21 lies in the vicinity of molecular clouds
- ⇒ [S II] but no [O III] ⇒ $v_{shock} < 100$ km s^{-1}, densities 2.5 cm^{-3} (Mavromatakis et al., 2007)
- ⇒ shocked CO filaments (densities $\sim 10^2 - 10^4$ cm^{-3} and filling factors ≤ 0.1, Koo et al., 2001)
- ⇒ HI density for expanding shell: ~ 8 cm^{-3} (Koo et Heiles, 1991)
- ⇒ maximum density (volume-average) = 25 cm^{-3}

Emission mechanism

- ⇒ hadronic scenario
  - ↪ π^0-decay
- ⇒ leptonic scenario
  - ↪ IC scattering
  - ↪ non-thermal Bremsstrahlung emission (dominates over IC for large density as in HB 21)

One-zone model

emitting zone = best fit γ-ray disk

nuclei and electrons described by: $\frac{dN}{dp} \propto \eta_{e,p} p^{-\Gamma} e^{-\frac{p}{p_{max}}}$

One-zone model

emitting zone = best fit γ-ray disk

nuclei and electrons described by: $\frac{dN}{dp} \propto \eta_{e,p} p^{-\Gamma} e^{-\frac{p}{p_{max}}}$

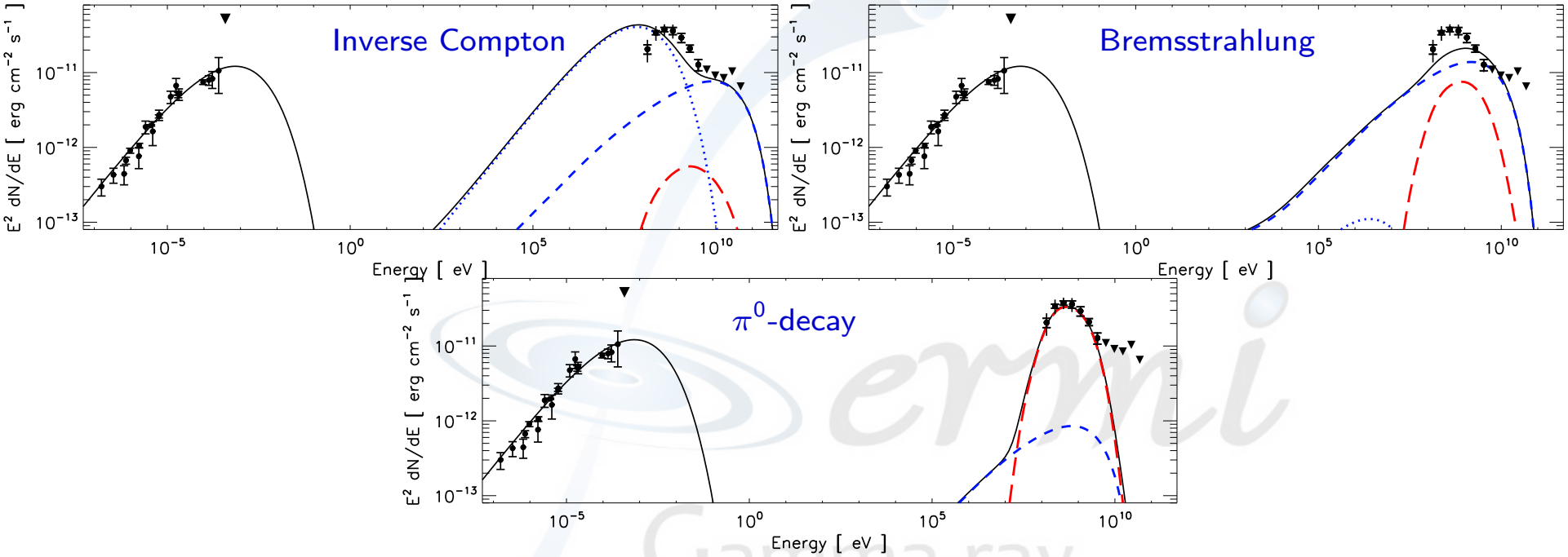

Model	Index	$p_{\rm max}$	$n_{\rm H}$	$B_{\rm tot}$	η_e/η_p	W_p	W_e
		[GeV/c]	[cm^{-3}]	[μG]		[erg]	[erg]
IC	1.76	100	0.1	2	1	1.3×10^{50}	2.1×10^{51}
Brems.	1.76	19	15	24	6.4	$\times10^{48}$	3.0×10^{48}
π^0-decay	1.76	8.1	15	140	0.001	3.0×10^{49}	1.1×10^{47}

Two-zone model

zone 1 $\rightarrow$ dense filaments $\rightarrow$ $n = 500$ cm^{-3}, filling factor $= 0.03$ $\rightarrow$ γ-ray emission

zone 2 $\rightarrow$ $n = 1$ cm^{-3}, $B = 50$ μG $\rightarrow$ radio emission

Two-zone model

zone 1 → dense filaments → $n = 500$ cm^{-3}, filling factor = 0.03 → γ-ray emission

zone 2 → $n = 1$ cm^{-3}, $B = 50$ μG → radio emission

Bremsstrahlung

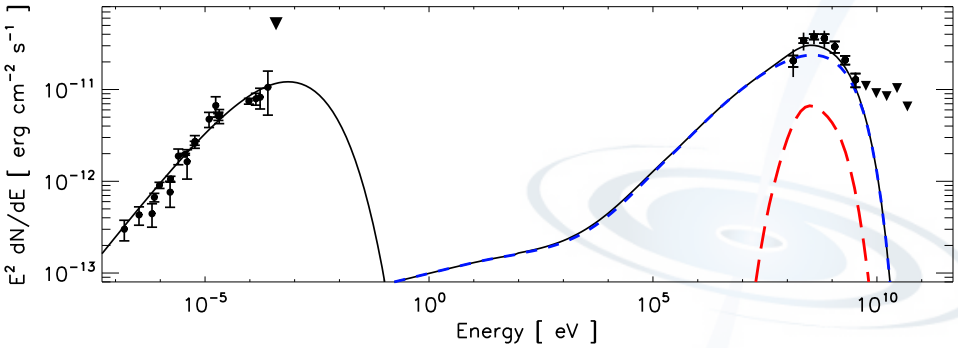

π^0-decay

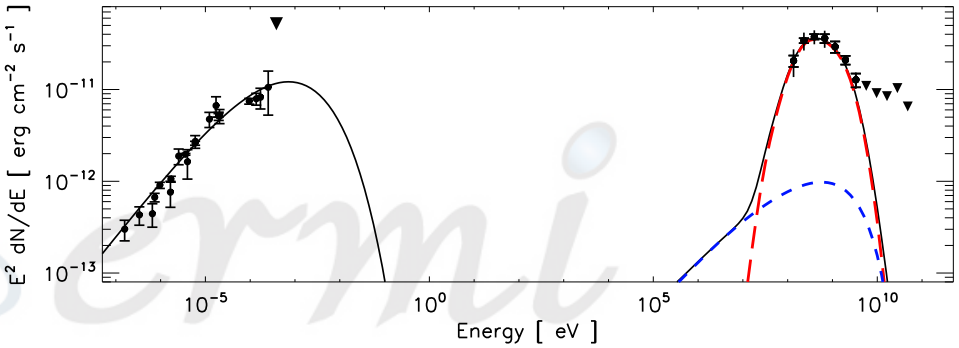

Model	Index	$p_{\max}$ [GeV/c]	$n_{\rm H}$ [cm^{-3}]	$B_{\rm tot}$ [μG]	η_e/η_p	W_p [erg]	W_e [erg]
Brems.	1.76	4	1.76	8	0.1	6.7×10^{48}	3.2×10^{48}
π^0-decay	2.0	9	1.76	4	0.001	3.5×10^{49}	1.6×10^{47}

possible Bremsstrahlung origin of γ-ray emission from dense filaments, BUT not well constrained by data

Comparison with other SNRs detected by Fermi LAT

characteristic	HB 21	other SNR
luminosity	$(3.3 \pm 0.6) \times 10^{34}$ erg s^{-1}	$\geq 10^{35}$ erg s^{-1} (IC443)
mass shocked clouds	$\sim 3000\ M_\odot$ [a]	$> 10^4\ M_\odot$ (IC 443 and W44)

[a] Byun et al. (2006)
[b] Katagiri et al. (2011)
[c] Abdo et al. (2010)

Comparison with other SNRs detected by Fermi LAT

characteristic	HB 21	other SNR
luminosity	$(3.3 \pm 0.6) \times 10^{34}$ erg s^{-1}	$\geq 10^{35}$ erg s^{-1} (IC443)
mass shocked clouds	$\sim 3000\ M_\odot$ [a]	$> 10^4\ M_\odot$ (IC 443 and W44)
radio index	flat	flat (IC 443 and W 44)

[a] Byun et al. (2006)
[b] Katagiri et al. (2011)
[c] Abdo et al. (2010)

Possible explanation

- ⇒ ionization losses (Leahy, 2006)
- ⇒ low-frequency absorption by thermal electrons (Leahy, 2006)
- ⇒ re-acceleration takes place in the compressed cloud (Uchiyama et al., 2010)

Comparison with other SNRs detected by Fermi LAT

characteristic	HB 21	other SNR
luminosity	$(3.3 \pm 0.6) \times 10^{34}$ erg s^{-1}	$\geq 10^{35}$ erg s^{-1} (IC443)
mass shocked clouds	$\sim 3000\ M_\odot$ [a]	$> 10^4\ M_\odot$ (IC 443 and W44)
radio index	flat	flat (IC 443 and W 44)
cutoff or break in γ-ray	yes	Cygnus Loop [b], W28[c]

[a] Byun et al. (2006)
[b] Katagiri et al. (2011)
[c] Abdo et al. (2010)

Possible explanation

- ⇒ runaway cosmic rays illuminating nearby clouds (Gabici et al., 2009)
- ⇒ re-acceleration in highly-compressed shocks (Uchiyama et al., 2010)
- ⇒ magnetic damping of Alfven waves in a partially ionized medium (Malkov et al., 2011)

Conclusions

no spectral variations found

Conclusions

no spectral variations found

curved spectrum indicative of a cutoff or break

Conclusions

no spectral variations found

curved spectrum indicative of a cutoff or break

low total luminosity due to lower mass of the interacting molecular clouds but in agreement with the value obtained by Reichardt et al. (2012)

Conclusions

no spectral variations found

curved spectrum indicative of a cutoff or break

low total luminosity due to lower mass of the interacting molecular clouds but in agreement with the value obtained by Reichardt et al. (2012)

curved radio spectrum

Conclusions

no spectral variations found

curved spectrum indicative of a cutoff or break

low total luminosity due to lower mass of the interacting molecular clouds but in agreement with the value obtained by Reichardt et al. (2012)

curved radio spectrum

γ-ray emission dominated by the π^0-decay

Conclusions

no spectral variations found

curved spectrum indicative of a cutoff or break

low total luminosity due to lower mass of the interacting molecular clouds but in agreement with the value obtained by Reichardt et al. (2012)

curved radio spectrum

γ-ray emission dominated by the π^0-decay

total energy of $\sim 3 \times 10^{49}$ erg

Backup slides

How to calculate systematic errors on morphology

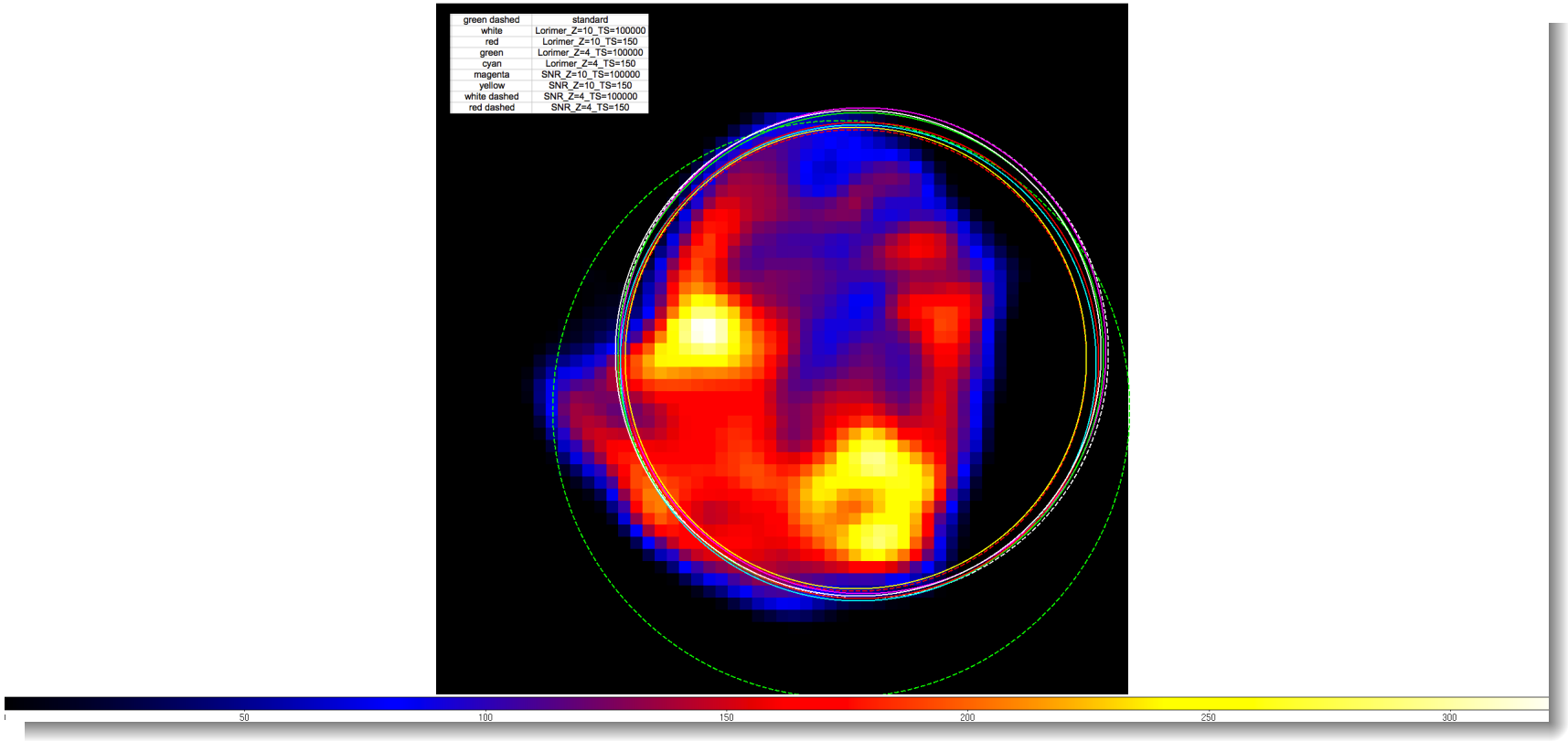

Systematic errors: disk shifted toward north-western part

shifts in longitude between $0^{\circ}.19$ and $0^{\circ}.24$, and in latitude between $0^{\circ}.06$ and $0^{\circ}.09$

the radius is smaller by $0^{\circ}.18$ - $0^{\circ}.24$

How to calculate systematic errors on spectrum

Systematic errors

⇒ Effective area (EA)

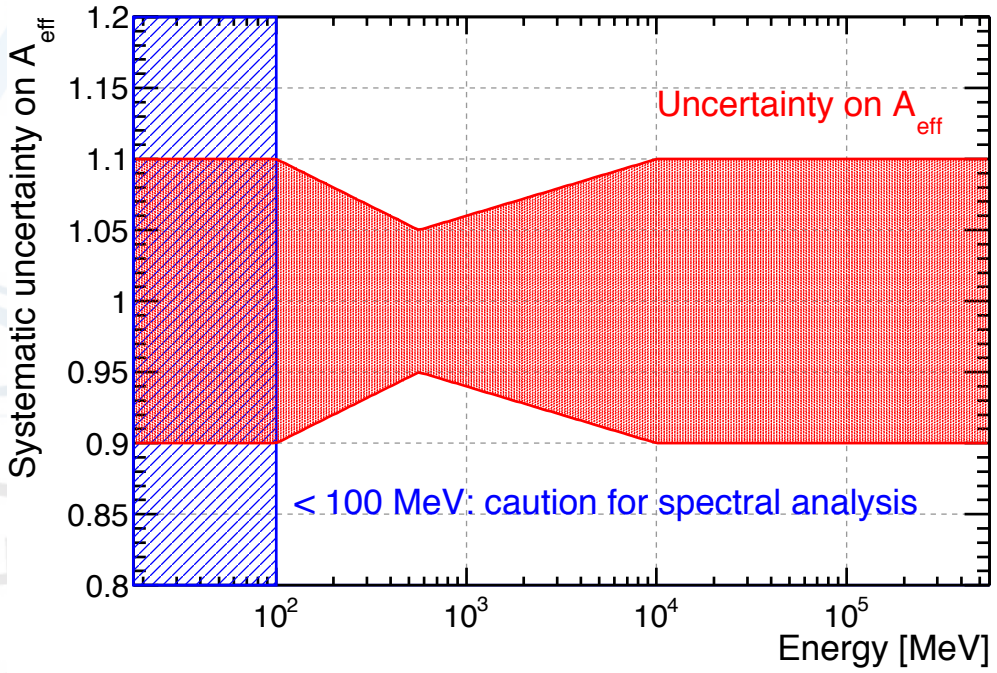

How to calculate systematic errors on spectrum

Alternative models developed by:

F.de Palma, G.Johannesson, L.Tibaldo, T.J.Brandt, J.Ballet, J.W.Hewitt, and F.Acero

Systematic errors

- ⇒ Effective area (EA)
- ⇒ Interstellar emission model (ISM)

Compare results obtained with 8 different models changing

- ⇒ spin temperature of atomic hydrogen (150 K and 10^5 K)
- ⇒ height of CR propagation halo (4 kpc and 10 kpc)
- ⇒ CR source distribution in the Galaxy (Lorimer (2006) and SNR distribution by Case&Bhattacharya (1998))

$$\sigma_{EA,ISM} = \sqrt{\frac{\sum_{i=1}^{n_{alt}} (x_{alt} - x_{standard})^2}{n_{alt}}}$$

$$\sigma_{tot} = \sqrt{\sigma_{EA}^2 + \sigma_{ISM}^2}$$